ANZIAM J. **63** (2021), 84–99
doi:10.1017/S1446181121000080

ANALYSIS OF CELL TRANSMISSION MODEL FOR TRAFFIC FLOW SIMULATION WITH APPLICATION TO NETWORK TRAFFIC

A. S. MAULANA[1] and S. R. PUDJAPRASETYA[1]

(Received 5 January, 2020; accepted 6 March, 2021; first published online 18 May, 2021)

Abstract

The cell transmission model (CTM) is a macroscopic model that describes the dynamics of traffic flow over time and space. The effectiveness and accuracy of the CTM are discussed in this paper. First, the CTM formula is recognized as a finite-volume discretization of the kinematic traffic model with a trapezoidal flux function. To validate the constructed scheme, the simulation of shock waves and rarefaction waves as two important elements of traffic dynamics was performed. Adaptation of the CTM for intersecting and splitting cells is discussed. Its implementation on the road segment with traffic influx produces results that are consistent with the analytical solution of the kinematic model. Furthermore, a simulation on a simple road network shows the back and forth propagation of shock waves and rarefaction waves. Our numerical result agrees well with the existing result of Godunov's finite-volume scheme. In addition, from this accurately proven scheme, we can extract information for the average travel time on a certain route, which is the most important information a traveller needs. It appears from simulations of different scenarios that, depending on the circumstances, a longer route may have a shorter travel time. Finally, there is a discussion on the possible application for traffic management in Indonesia during the Eid al-Fitr exodus.

2020 *Mathematics subject classification*: primary 35L67; secondary 65M06.

Keywords and phrases: cell transmission model, kinematic wave model, method of characteristics, junction.

1. Introduction

Some major cities in Indonesia are suffering from a lack of roads. According to Boel and Mihaylova [1], city roads should ideally account for about 25% of the total area of

[1] Industrial and Financial Mathematics Research Group, Faculty of Mathematics and Natural Sciences, Institut Teknologi Bandung, Jalan Ganesha 10, Bandung 40132, Indonesia;
e-mail: adysulton@gmail.com, sr_pudjap@math.itb.ac.id

the city, with a minimum of about 15%. However, most major cities in Indonesia have less road area than the minimum standard, such as Bandung, which has only about 10%. Without proper public transport, the densely populated cities of Indonesia are experiencing serious traffic congestion problems. In order to reduce traffic congestion, traffic flow needs to be maximized, and engineers have to determine whether to turn a two-way street into a one-way street, where to build entrances, exits or overpasses, and so on. In order to make such decisions, engineers simulate possible scenarios using simulation packages.

Although traffic simulation packages have existed since the 1960s [13], modelling and numerical simulation of traffic still remain an active area of research. One widely used numerical model is the cell transmission model (CTM) which was first proposed by Daganzo [3] and Lebacque [8], and later reviewed by Orosz et al. [12]. Accurate calculations of traffic inflows and outflows via junctions are required for the simulation of traffic dynamics in a network, and therefore an efficient and robust model is a very important element. To provide an overview of CTM-related studies at junctions, we provide a short list of literature reviews. Zhang et al. [18] implemented the CTM to predict spatial queuing characteristics behind a bottleneck, comparing the results to two other methods. They showed that CTM predicted traffic congestion in accordance with results from deterministic theory. The simulation of traffic jam growth and dispersal by Long et al. [10] has been used to develop traffic management strategies. Furthermore, the method has been integrated into a hybrid system called the switching mode model, which was used by Muñoz et al. [11] and Gomez et al. [6] in ramp metering control system for highways. Discussions on the stochastic version of the CTM were conducted by Boel and Mihaylova [1] and Sumalee et al. [16]. The extension of the original CTM by incorporating various shapes of fundamental diagrams was discussed by Chen et al. [2].

The effectiveness and accuracy of the CTM are examined in this paper. The discussion in Section 2 begins with a finite-volume approximation of the kinematic Lighthill–Whitham–Richards (LWR) equation using a triangular or trapezoidal flux–density relationship; we show that this is nothing more than the formula of the CTM. In Section 3 the scheme is tested using the exact solution of the kinematic LWR equation, that is, the shock wave and rarefaction wave. However, since the flux function is trapezoidal, that is, a piecewise differentiable function, the CTM rarefaction wave is also a discontinuous solution. Section 4 discusses the adaptation of CTM to model fluxes for diverging and merging streams, followed by a validation using the analytical solution of kinematic model. In Section 5 the numerical simulation of traffic dynamics in a simple road network is carried out; the results show the back and forth propagation of shock waves and rarefaction waves, which confirms the result of the Godunov method by Wenlong [17]. In Section 6 the average travel time for vehicles taking different routes is calculated and analysed. Finally, we discuss one possible application for traffic management in Indonesia during the Eid al-Fitr exodus, and Section 7 concludes the paper.

https://doi.org/10.1017/S1446181121000080 Published online by Cambridge University Press

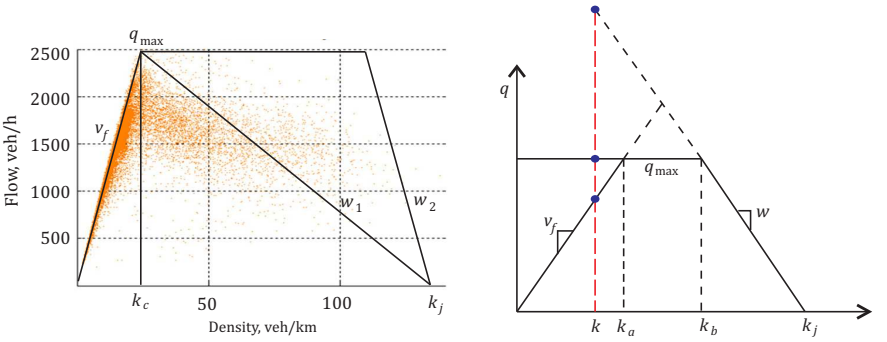

FIGURE 1. (Left) Plots of empirical traffic data from Ni [5] together with trapezoidal and triangular flux models. (Right) Illustration of formula (2.3) that actually computes flux q according to the trapezoidal flux model. (Colour available online.)

2. The cell transmission model

If $k(x,t)$ is the traffic density and $q(x,t)$ is the traffic flux, then car conservation requires that

$$\partial_t k + \partial_x q = 0, \tag{2.1}$$

which is often referred to as the LWR equation. Traffic flow models normally assume a prescribed relationship between flux and density $q = q(k)$ determined empirically. It is observed that for small to moderate traffic density, the flux increases linearly with density and reaches a maximum value after which the profile flattens out (see Figure 1 (left)). For higher densities the profile is linearly decreasing to zero at the maximum density possible on the road.

Consider Figure 1 (left). When traffic density is rather low, traffic flux can be well represented as a linear function $q = v_f k$. In that situation, most vehicles can move freely with a relatively constant speed v_f. For heavy traffic density, one can use linear regression to get the line with negative gradient $-w_i$, $i = 1, 2$, which intersects the horizontal axis at jam density k_j. The trapezoidal function used to model this behaviour (see Figure 1), consists of three straight lines: $v_f k$, $q_{\max}$, and $w_i(k_j - k)$ with $-w_i < 0$. Here $q_{\max}$ denote the maximum flux. When $|w_i|$ is relatively small, the trapezoid becomes a triangle, and the triangular flux function has parameters $q_{\max}, v_f, w_1, k_c, k_j$ (see Figure 1 (left)), with k_c the critical density. Explicitly, the flux function used is given by

$$q(k) = \begin{cases} v_f k & \text{for } 0 \le k \le k_a, \\ q_{\max} & \text{for } k_a < k \le k_b, \\ w(k_j - k) & \text{for } k_b < k \le k_j, \end{cases} \tag{2.2}$$

https://doi.org/10.1017/S1446181121000080 Published online by Cambridge University Press

(see Figure 1 (right)). The value of $q(k)$ as given in (2.2) can be obtained simply by using

$$q = \min\{v_f k, q_{\max}, w(k_j - k)\} \quad \text{for all } k \in [0, k_j]. \tag{2.3}$$

In numerical implementations, the computational domain is divided into cells of length Δx denoted by $C_{i-1}, C_i, C_{i+1}, \ldots$. We denote by $k_i(t)$ (veh/km) the traffic density in cell C_i at time t, and by $q_i(t)$ (veh/hour) the traffic flux entering cell C_i. Here we use "veh" (vehicles) as a unit. The finite-volume discrete form of the kinematic LWR model (2.1) reads

$$\frac{k_i(t + \Delta t) - k_i(t)}{\Delta t} = -\frac{q_{i+1}(t) - q_i(t)}{\Delta x}. \tag{2.4}$$

If we further denote

$$k_i(t)\Delta x \equiv n_i(t), \quad q_i(t)\Delta t \equiv f_i(t),$$

the discrete equations (2.4) and (2.3) become

$$n_i(t + \Delta t) = n_i(t) + f_i(t) - f_{i+1}(t), \tag{2.5}$$

$$f_i(t) = \min\{n_{i-1}(t), q_{\max}\Delta t, M - n_i(t)\}, \tag{2.6}$$

respectively, using $\Delta x = v_f \Delta t$ and $M = k_j \Delta x$. Here M (veh) denotes the maximum capacity of each cell. Equation (2.5) is exactly the CTM, also known as the supply and demand method. In that equation, variables n_i and f_i represent the total number of vehicles in cell i, and the total number of vehicles that can enter cell i, respectively, within time interval Δt (see Figure 2). An alternative form of the CTM flux (2.6) is

$$\begin{aligned} f_i(t) &= \min\{D_{i-1}, S_i\}, \\ D_{i-1} &= \min\{n_{i-1}(t), q_{\max}\Delta t\}, \\ S_i &= \min\left\{q_{\max}\Delta t, \frac{w}{v_f}(k_j \Delta x - n_i(t))\right\}, \end{aligned}$$

where D_{i-1} represents demand (the sending flow into C_i) and S_i represents supply (the receiving flow by C_i), respectively. In this respect, the actual flux $f_i(t)$ is determined by demand D_{i-1} and supply $S_i(t)$, which explains the origin of the name "supply and demand method". An application of the finite volume method (2.4) with the parabolic flux function for traffic flow with traffic light, was discussed by Pudjaprasetya et al. [14].

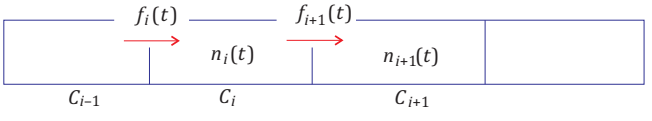

FIGURE 2. Illustration of the CTM formula (2.5).

https://doi.org/10.1017/S1446181121000080 Published online by Cambridge University Press

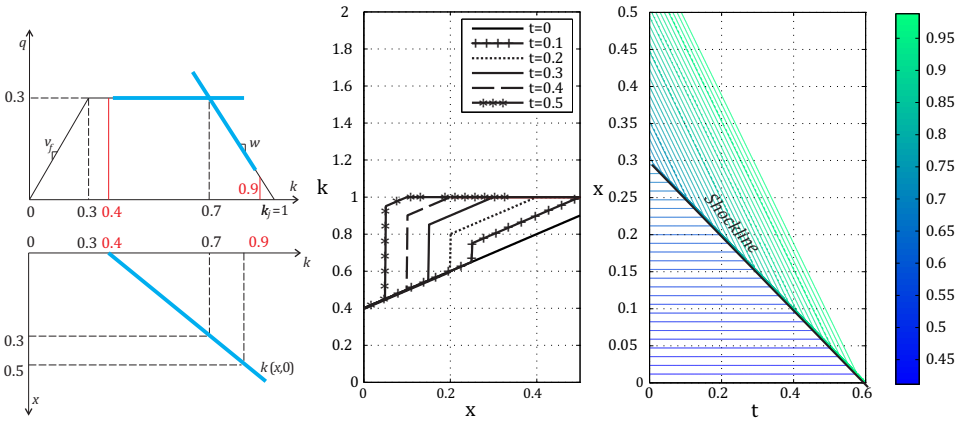

FIGURE 3. (Left) Initial density $k(x, 0)$ and the trapezoidal flux (2.2). (Middle) Snapshot of the numerical $k(x, t)$ at subsequent times, showing a shock wave propagating backwards. (Right) Contour plot of the numerical $k(x, t)$ and the shock line.

3. Numerical validation

Here we check the accuracy of the CTM model (2.5) and (2.6) by examining situations for which there are exact solutions. We use the trapezoidal flux (2.2) described earlier, with normalized parameters $v_f = k_j = w = 1$ and $q_{\max} = 0.3$, and consequently $k_a = 0.3$ and $k_b = 0.7$. Gradients of the characteristic lines is given by the gradient of the flux function, so for this trapezoidal flux there are just three possible values: v_f, $-w$ and zero. Hence, the analytical shock wave and rarefaction wave solutions of (2.1) can be easily sketched using the method of characteristics.

3.1. Shock waves We first examine a shock wave situation corresponding to an initial density distribution given by

$$k(x, 0) = 0.4 + x, \tag{3.1}$$

on the computational domain $0 \le x \le 0.5$. According to the flux function (2.2), the initial density (3.1), which gives $0.4 \le k(x, 0) \le 0.9$, has two families of characteristic lines: those with zero gradient for $0.3 < k(x, 0) < 0.7$, with $x < 0.3$; and those with negative gradient $-w = -1$ for $k(x, 0) > 0.7$, with $x > 0.3$ (see Figure 3 (left)). In the (x, t)-plane, the two sets of characteristic lines intersect, indicating the occurrence of a shock wave solution. A shock wave will propagate following a shock line with a gradient given by the Rangkine–Hugoniot condition [9], that is, the average gradient of the two characteristic sets -0.5.

Next, the numerical CTM (2.5)–(2.6) was implemented, and the result is given in Figure 3 (middle, right). We can observe that part of the initial wave with density $k > 0.7$ propagates to the left with velocity -1, and the other part, with initial density $0.4 < k < 0.7$, remains steady (zero velocity). The outcome is a shock wave with a shock front that propagates with velocity $(-1 + 0)/2 = -0.5$. This same result is obtained

https://doi.org/10.1017/S1446181121000080 Published online by Cambridge University Press

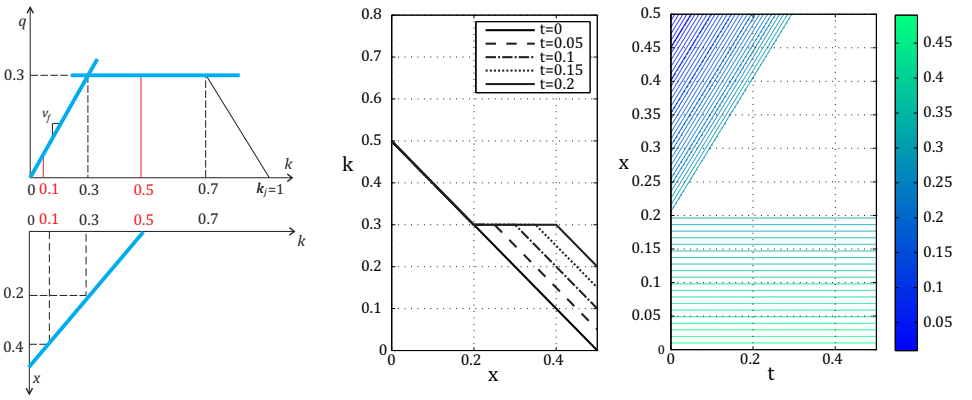

FIGURE 4. (Left) Initial density $k(x,0)$ and trapezoidal flux (2.2). (Middle) Snapshot of the numerical $k(x,t)$ at subsequent times, showing a rarefaction wave propagating forwards. (Right) Contour plot of the numerical $k(x,t)$.

from the exact analytic solution; the numerical scheme correctly captures the traffic behaviour in this case.

3.2. Rarefaction waves The second simulation is a rarefaction wave, which corresponds to the initial density

$$k(x,0) = 0.5 - x,$$

on the computational domain $0 \le x \le 0.5$, which gives $0 \le k(x,0) \le 0.5$. The part with $k(x,0) > 0.3$ has characteristic lines with zero gradient, whereas the part with $k(x,0) < 0.3$ has characteristic lines with positive gradient $v_f = 1$ (see Figure 4 (left)). Instead of intersecting each other, the two families of characteristics go farther and farther apart, leaving an empty wedge-shaped area in between. The CTM result in Figure 4 (middle) shows that part of the initial density with $k(x,0) > 0.3$ is unchanged, while the other part with $k(x,0) < 0.3$ moves with velocity $v_f = 1$, exactly in agreement with the characteristic lines analysis. A snapshot of the traffic density at subsequent times in Figure 4 (middle) shows the rarefaction wave produced by CTM, which is not a smooth transition solution.

4. Splitting and merging streams

In this section we discuss situations in which traffic streams split or merge. We adopt the modified CTM formula by Daganzo [4] for cells which merge and diverge, which will be recalled here for clarity. The case with merging streams will be validated using the analytical solution of the kinematic LWR model (2.1).

4.1. Merging streams Suppose two roads intersect at a junction, so that vehicles from the two cells C_{i-1}, C'_{i-1} enter the single cell C_i (see Figure 5 (left)). Suppose that at time step t_j traffic demands from the two upstream cells C_{i-1} and cell C'_{i-1} are D_{i-1}

https://doi.org/10.1017/S1446181121000080 Published online by Cambridge University Press

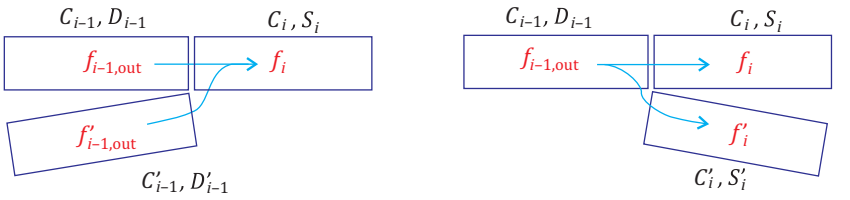

FIGURE 5. (Left) A merging cell C_i which receives fluxes from cell C_{i-1} and C'_{i-1}. (Right) A diverging cell C_{i-1} sending traffic fluxes to cells C_i and C'_i.

and D'_{i-1}, respectively, whereas the supply of the downstream cell C_i is S_i. Let $f_{i-1,\text{out}}$ and $f'_{i-1,\text{out}}$ denote the actual outflow from C_{i-1} and C'_{i-1}, respectively. Clearly,

$$f_i = f_{i-1,\text{out}} + f'_{i-1,\text{out}}. \tag{4.1}$$

Further, we adopt the formula by Daganzo [4] as follows:

$$f_{i-1,\text{out}} = D_{i-1}, f'_{i-1,\text{out}} = D'_{i-1} \quad \text{if } D_{i-1} + D'_{i-1} \le S_i, \tag{4.2}$$

$$f_{i-1,\text{out}} = pS_i, f'_{i-1,\text{out}} = (1-p)S_i \quad \text{if } D_{i-1} + D'_{i-1} > S_i, \tag{4.3}$$

where p, the proportional demand of the two legs, is given by

$$p = \frac{D_{i-1}}{D_{i-1} + D'_{i-1}}. \tag{4.4}$$

Formula (4.2) means that if the total demand is less than or equal to the supply, then all vehicles from both upstream legs enter cell C_i and move freely. If, however, the demand is greater than the supply, then only a proportion of the supply can be accommodated, that is, formula (4.3) applies. To calculate the traffic distribution in a road section with such merging circumstances, the influx into the merging cell C_i is replaced with (4.1)–(4.4). This modification is applied only for the merging cell, while for other cells the actual flow follows from (2.6). We now examine a simple simulation to test this CTM modification.

Consider a road segment of length 1 km, and take the initial zero traffic density $k(x, 0) = 0$. In the region $0 < x < x_E = 0.2$, vehicles enter at a constant rate β_0 (veh/km). The change in traffic density as time progresses is computed using the CTM with a triangular flux function with parameters $v_f = 1$ km/min, $-w = -0.3$ km/min, $k_j = 180$ veh/km.

The CTM result in Figure 6 shows the effect of low influx $\beta_0 = 207$ veh/km. As a response to the positive influx, traffic density in the entrance region starts to increase, as time progresses it continues to increase until it reaches the maximum of $k_c = 41.5385$ veh/km. As shown in Figure 6 (left), the CTM result confirms the analytical solution of the kinematic model [7].

For a high influx, the characteristic method predicts that a shock wave will start to emanate from the end of the entrance region $x = x_E$. This shock wave then propagates

https://doi.org/10.1017/S1446181121000080 Published online by Cambridge University Press

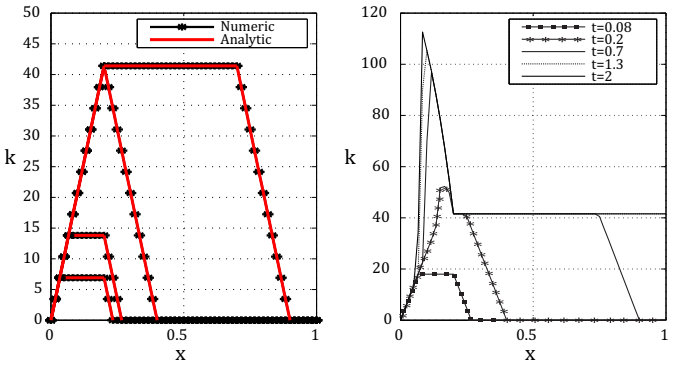

FIGURE 6. Snapshot of the traffic density, (left) under the influence of a constant influx $\beta_0 = 207$, validated using the analytical solution, and (right) with traffic influx $\beta_0 = 265$, in which a backward-propagating shock wave appears.

backwards (to the left). According to Haberman [7], the shock wave will form if β_0 satisfies

$$\beta_0 \geq \beta_c \quad \text{with } \beta_c \equiv \frac{v_f k_c}{x_E}.$$

In our simulation, we use parameters $x_E = 0.2$, $v_f = 1$, $k_c = 0.3$, hence the critical value is $\beta_c = 207.6923$. By using the traffic influx $\beta_0 = 265 > \beta_c$, the CTM simulation shows a backward-propagating shock wave (Figure 6 (right)), just as predicted analytically. A detailed discussion of this aspect is given by Pudjaprasetya and Kamalia [15].

4.2. Splitting streams Consider a cell that splits into two cells as shown in Figure 5. Suppose that D_{i-1} denotes the demand of cell C_{i-1}, while S_i and S_i' denote the traffic supply of two downstream cells C_i and C_i', respectively. The actual outflow from cell C_{i-1} is denoted by $f_{i-1,\text{out}}$, whereas the actual inflows to the two downstream cells are f_i, f_i', respectively (see Figure 5 (right)).

We introduce a parameter α, with $0 \leq \alpha \leq 1$, that represents the proportion of vehicles choosing the C_i route. For instance, $\alpha = 1$ means all users choose to go to C_i, and none to go to C_i'. Consequently, the following relations hold:

$$\begin{aligned} &f_{i-1,\text{out}} = f_i + f_i' \quad \text{and } f_{i-1,\text{out}} \leq D_{i-1}, \\ &f_i = \alpha \times f_{i-1,\text{out}} \quad \text{and } f_i \leq S_i, \\ &f_i' = (1-\alpha) \times f_{i-1,\text{out}} \quad \text{and } f_i' \leq S_i'. \end{aligned} \tag{4.5}$$

Moreover, it is clear that

$$f_{i-1,\text{out}} = \min\left\{D_{i-1}, \frac{S_i}{\alpha}, \frac{S_i'}{(1-\alpha)}\right\}. \tag{4.6}$$

Implementation of the CTM scheme with a diverging cell needs a predefined α. This will be discussed in the next section, where it is applied to a simple traffic network.

https://doi.org/10.1017/S1446181121000080 Published online by Cambridge University Press

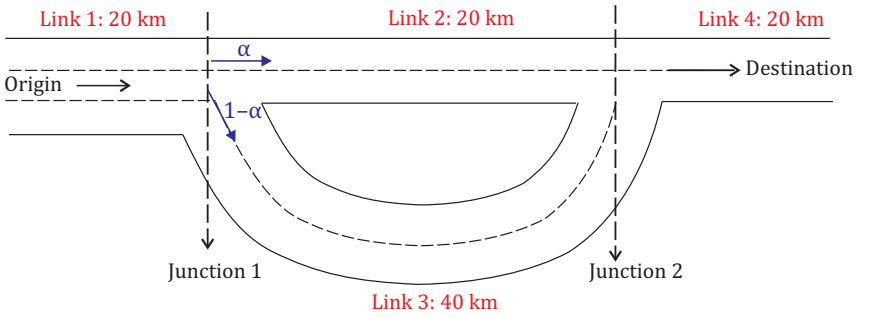

FIGURE 7. A simple road network, used in CTM simulation using the diverged parameter α.

5. Simulation of a simple traffic network

In this section, the CTM method is implemented to compute the traffic distribution in a simple road network. Figure 7 shows the simple road network consisting of four links that are connected using two junctions. Assume that all vehicles departing from the origin intend to reach the destination without stopping. At Junction 1, they have two options: whether to take Link 2 or Link 3; both links will lead them to Junction 2 at which both links merge into Link 4. Links 1, 2, and 4 all have the same length of 20 km, whereas Link 3 is 40 km in length. Furthermore, Link 1 has three lanes, while the other links have two lanes.

In our simulation, the following triangular flux function is adopted:

$$q(\ell, k) = \begin{cases} v_f k & \text{for } \ 0 \le k \le \ell k_c, \\ w(\ell k_j - k) & \text{for } \ \ell k_c \le k \le \ell k_j, \end{cases}$$

with parameters jam density $k_j = 180$ veh/km/lane, free flow speed $v_f = 65$ km/hr, and backward wave speed $-w = -16.25$ km/hr, consequently $q_{\max} = 2340$ veh/hr/lane. Parameter ℓ denotes the number of lanes, and $k_c = 36$ veh/km/lane denotes the critical density. For this triangular flux function, $k < k_c$ represents the uncongested condition, whereas $k > k_c$ represents the congested condition. Within the uncongested region, shock waves and rarefaction waves propagate to the right with velocity v_f, whereas within the congested region, those waves propagate to the left with velocity w.

Initially, the road is empty with density $k(x, 0) = 0$. For the first six hours $t \in [0, 6]$, we assume that there is a constant traffic supply with flux $3q_{\max}$, and zero after that, so that

$$k(0, t) = \begin{cases} 3q_{\max} & 0 \le t \le 6, \\ 0 & t > 6. \end{cases}$$

At the destination, the traffic supply (receiving flow) is always the capacity of two lanes. Computation is conducted using time-step $\Delta t = 2.52$ seconds $= 0.0007$ hr, so $\Delta x = v_f \Delta t = 0.0455$ km $= 45.5$ m. For the diverging cell at Junction 1 (Figure 7) we implemented (4.5)–(4.6) with $\alpha = 0.7$, whereas for the merging cell at Junction

https://doi.org/10.1017/S1446181121000080 Published online by Cambridge University Press

2 (Figure 7), we used (4.1)–(4.3). Simulation results are shown in Figure 8, in which the traffic density contours for each link were plotted as functions of spatial variable x and time t.

To describe the traffic dynamics occurring in the simulation, the whole process is divided into three phases. Phase I begins when vehicles enter the road network with speed v_f, and arrive at Junction 1 at $t_1 = 20/v_f$ hr. At Junction 1, the outflux of Link 1 is counted using equation (4.6),

$$f_{1,\text{out}} = \min\left\{3q_{\max}, \frac{2q_{\max}}{0.7}, \frac{2q_{\max}}{0.3}\right\} = \frac{20}{7}q_{\max}.$$

So, the influx to Link 2 is $0.7f_{1,\text{out}} = 2q_{\max}$, and the influx to link 3 is $0.3f_{1,\text{out}} = \frac{6}{7}q_{\max}$. Next, for $t > t_1$, on Links 2 and 3, density propagates to the right with speed v_f. While at Junction 1, a shock wave is formed and propagates to the left on Link 1 with speed

$$\frac{3q_c - (20/7)q_c}{k(3q_c) - k((20/7)q_c)} = -w.$$

These two right-propagating shock waves can be observed in Figure 8 as straight lines with gradient $1/v_f$, emerging from Junction 1, on Links 2 and 3. At time $t_2 = t_1 + (20/v_f)$, the first vehicle on Link 2 arrives at Junction 2. Based on equation (4.2), the influx to Link 4 is

$$f_{4,in} = \min\{2q_{\max}, 2q_{\max}\} = 2q_{\max}.$$

Phase II starts at time $t_3 = t_1 + (40/v_f)$ hr, that is, when the first vehicle on Link 3 arrives at Junction 2. Because vehicles on Link 3 have entered Link 4, the outflux of Link 2 has decreased, and consequently a shock wave forms at Junction 2 and propagates to the left with speed

$$\frac{2q_{\max} - (\frac{7}{10})2q_{\max}}{k(2q_{\max}) - k((\frac{7}{10})2q_{\max})} = -w.$$

In Figure 8, this backward-propagating shock wave on Link 2 appears as a line with negative gradient $-1/w$. When this shock wave arrives at Junction 1 at $t_4 = t_3 + (20/w)$ hr, it reduces the outflux of Junction 1, that is, $f_{1,\text{out}}$. Based on (4.6), the reduced $f_{1,\text{out}}$ will induce a shock wave that will propagate to the left on Link 1, as well as a reduced density that will propagate to the right on Link 3. This reduced density on Link 3 arrives at Junction 2 when $t_5 = t_4 + (40/v_f)$ hr. Based on equation (4.3), after t_5, the density at the end of Link 2 is reduced, hence a rarefaction wave is formed and propagates to the left. These back and forth phenomena continue between Junction 1 and 2.

Phase III starts at $t_8 = 6$ hr, which is when no more vehicles are entering the road network from the origin. The shock wave propagates at Link 1, forwards onto Links 2 and 3. At Link 3, the shock wave propagates with speed v_f, while at Link 2 it travels slowly.

https://doi.org/10.1017/S1446181121000080 Published online by Cambridge University Press

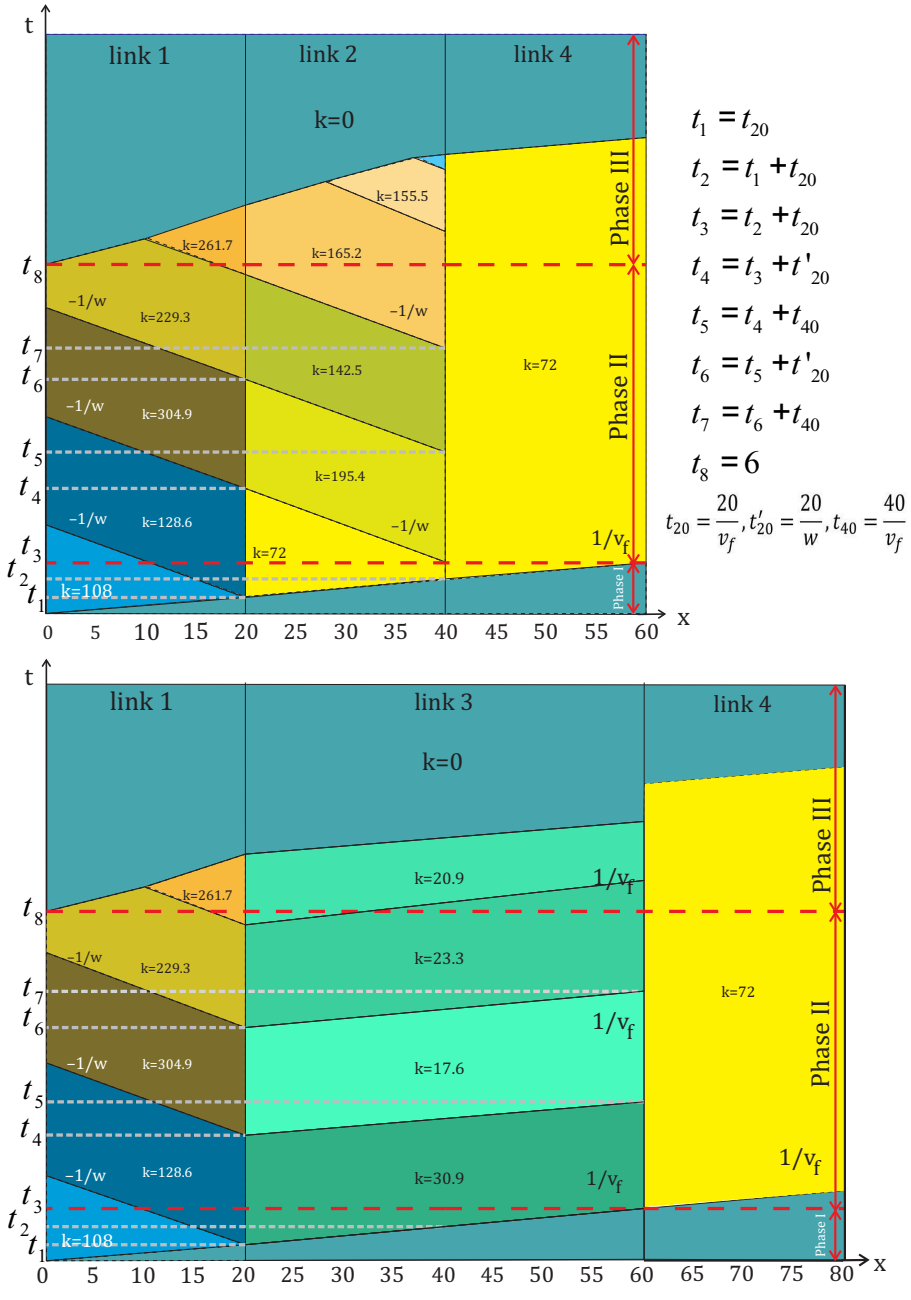

FIGURE 8. Contours of traffic density in Links 1–2–4 (top) and Links 1–3–4 (bottom), resulting from CTM simulation using the diverged parameter $\alpha = 0.7$.

https://doi.org/10.1017/S1446181121000080 Published online by Cambridge University Press

In summary, we can see that, starting from a zero initial condition and a simple boundary condition, our CTM method can compute traffic dynamics on a simple network. The result shows the back and forth propagation of shock waves and rarefaction waves. If the downstream density is larger than the upstream, a shock wave will emanate, otherwise a rarefaction wave will result. These waves travel with velocity v_f or $-w$, depending on whether the traffic density was in uncongested or congested regions, respectively (see Figure 1 (right)). There were only two possibilities, v_f or $-w$, because we used a triangle flux function. Our result shows good agreement with similar computations using the Godunov method by Wenlong [17]. Compared to the Godunov method, the CTM is much simpler, allowing us to easily implement the CTM in a more complicated road network. In addition, from this simulation we can extract information about travel times. A way to do this is discussed in the next section.

6. Cumulative flow and travel time

Suppose $f^*(x_i, s)$ denotes the flow through a point x_i at time s. Then the cumulative flow, which is the total number of vehicles that pass through a point x_i for time interval $[0, t]$, is given by

$$N(x_{i-1/2}; [0, t]) = \int_{s=0}^{t} f^*(x_{i-1/2}, s)\, ds.$$

The cumulative flow curve is also known as the N-curve.

In Figure 9 (left) two N-curves $N(x_i; [0, t])$, $i = 1, 2$, are plotted. These two N-curves should be synchronized first, meaning that a certain vehicle N_0 passes x_1 at time t_1, and passes x_2 at time t_2. Then we can simply deduce the travel time of vehicle N_0 from x_1 to x_2 as just $t_2 - t_1$. Since the flow $f(x_{i-1/2}, t)$ is nonnegative, the $N-$ curve is nondecreasing, hence from $N(x_1; [0, t])$ we can obtain the time at which vehicle N_0 passes x_1 from

$$T(N_0; x_1) = \min_s \{s \mid N(x_1; [0, s]) = N_0\}.$$

Hence, the time needed by vehicle N_0 to travel from x_1 to x_2 is

$$T(N_0; [x_1, x_2]) = T(N_0, x_2) - T(N_0, x_1).$$

Then total travel time between x_1 to x_2 for a group of vehicles is

$$T([N_1, N_2]; [x_1, x_2]) = \sum_{M=N_1}^{N_2} T(M; [x_1, x_2]),$$

where N_1 is the first vehicle entering the road segment $[x_1, x_2]$, and N_2 the last. Then the average travel time from x_1 to x_2 for every vehicle is just

$$\overline{T}([N_1, N_2]; [x_1, x_2]) = \frac{T([N_1, N_2]; [x_1, x_2])}{N_2 - N_1}, \tag{6.1}$$

which is the average value of $T(N; [x_1, x_2])$ over the interval $N \in [N_1, N_2]$.

https://doi.org/10.1017/S1446181121000080 Published online by Cambridge University Press

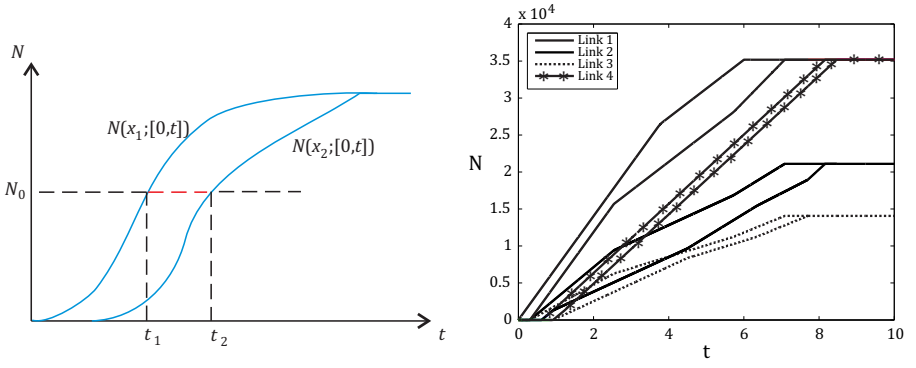

FIGURE 9. (Left) Illustration of two N-curves, which can be used to compute the average travel time from x_1 to x_2. (Right) Four pairs of N-curves resulting from the previous traffic network simulation using a diverged parameter $\alpha = 0.6$.

TABLE 1. Average travel time for each link in the road network in Figure 7. For all three scenarios, the average travel time of Link 2 and Link 3 is compared and the minimum written in bold.

	Average travel time		
	Scenario 1	Scenario 2	Scenario 3
Link 1	0.8	0.4	0.9
Link 2	1.201 676	**1.610 137**	**1.543 871**
Link 3	**0.749 043**	2.061 071	3.091 163
Link 4	0.3066	0.3066	0.3066

Using the concept of the average travel time discussed above, we reconsider the previous traffic dynamics in the road network of Figure 7. For this simulation, we will compare the average travel time via Link 2 and Link 3. First, we compute the N-curves for each link, and the results are depicted in Figure 9 (right). To be precise, the N-curves of Link 1 at the origin and at Junction 1 are represented in Figure 9 (right) as two red N-curves. From this pair of red N-curves, the average travel time at Link 1 can be computed using (6.1), and yield a value 0.8. Using the same procedure, the average travel time for Links 2–4 can also be computed, and the results are summarized in Table 1 (the second column). Unexpectedly, although Link 3 is twice as long as Link 2, the Link 3 travel time is shorter than the Link 2 travel time. Of course, this conclusion is strongly dependent on the specific parameters used in the simulation.

To complete the discussion, we conducted two additional scenarios; we designate the simulation discussed in Section 5 as Scenario 1. All three scenarios use the diverged parameter $\alpha = 0.6$. For Scenario 2, all parameters are kept the same, except that Link 2 now has three lanes. In Scenario 3, all parameters are the same as in Scenario 1, except that now there is an additional source in the middle part of Link 3.

https://doi.org/10.1017/S1446181121000080 Published online by Cambridge University Press

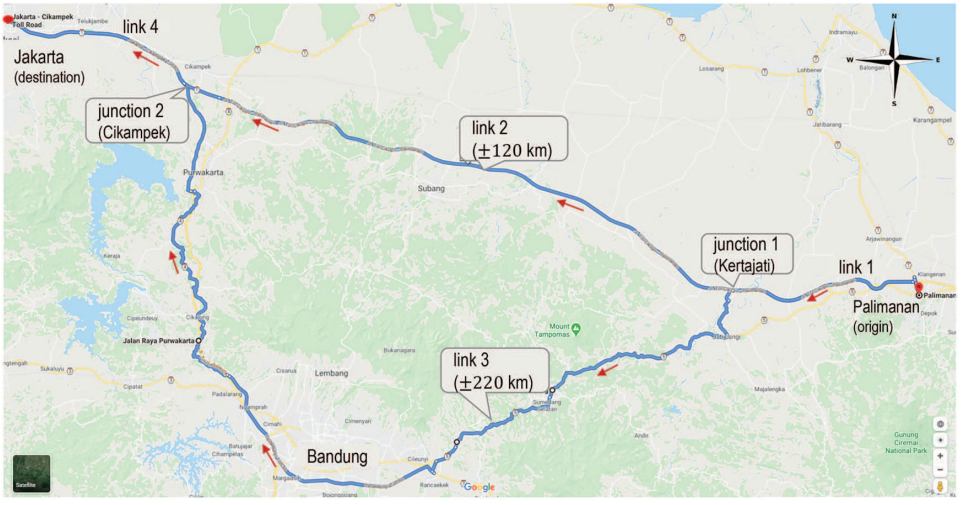

FIGURE 10. Palimanan–Jakarta road map via Link 2 or Link 3, (source: Google Maps).

For these two alternatives, similar computations were conducted. Focusing only on the average travel time, the results of Scenarios 2 and 3 compared with Scenario 1 in Table 1. If Link 2 has three lanes, taking Link 2 is recommended, since the average Link 2 travel time of is less than that of Link 3. However, if Link 2 has only two lanes, but there was an additional source with flux $2q_{\max}$ veh/hour in the middle of Link 3, taking Link 2 will take less time. To this end, the average travel time of a certain route can be calculated using a numerical model, thus helping traffic management to make recommendations on traffic arrangements.

The network case discussed above has direct relevance to the traffic situation on the Trans-Java Toll Road in Indonesia. A few days before Eid al-Fitr there will be a lot of traffic going east, and after Eid there will be even more traffic going west (backflow traffic). As shown in Figure 10, from Palimanan (origin) to Jakarta (destination), there are two options, via the Palimanan–Cikampek Toll Road (Link 2), or the longer road via Bandung (Link 3). To avoid heavy congestion during the heavy backflow traffic during Eid al-Fitr 2019, the government implemented a one-way system, combined with a contraflow policy for the road segment between Palimanan and Cikampek (Link 2). To explain the terms "one-way" and "contraflow", suppose Link 2 has four lanes. In normal situations four lanes are used for two-way traffic: two lanes for eastbound traffic, and the other two lanes for westbound traffic. In an emergency situation, this can be changed to using all four lanes for backflow traffic heading west (one-way system), or three lanes for westbound traffic and one lane for eastbound traffic (contraflow).

Traffic engineers must carry out an assessment of possible scenarios, as discussed above, prior to implementing such a change in traffic along the Palimanan–Cikampek

https://doi.org/10.1017/S1446181121000080 Published online by Cambridge University Press

road segment (Link 2). This includes the implementation of one-way traffic or contraflow. The aim is to avoid the accumulation of vehicles during the Eid exodus backflow. The CTM scheme proposed here is appropriate for this purpose, although a detailed assessment has not been discussed in this paper.

7. Conclusions

We discussed the relationship between the CTM and the finite-volume discretization of the kinematic LWR model with a trapezoidal flux function. Simulations of two classical solutions, shock waves and rarefaction waves, which precisely follow the analytical solution, supported the theoretical background of the CTM scheme. In addition, its agreement with the analytical solution for simulation in the case of merging streams, has demonstrated the accuracy of the CTM scheme. Moreover, its implementation on a simple network also confirms the existing results using the Godunov method. The average travel time for each road segment has also been calculated. This provides an example of analysing different route scenarios prior to the implementation of a traffic policy. The simplicity of the method and its ability to present traffic dynamics on traffic networks make the CTM a promising method for further development of traffic simulation packages.

Acknowledgements

We thank the reviewers for their comments and suggestions which helped improve and clarify this paper. Financial support from Indonesian Research Grant is greatly acknowledged.

References

[1] R. Boel and L. Mihaylova, "A compositional stochastic model for real time freeway traffic simulation", *Transport. Res. B-Meth.* **40** (2006), 319–334; doi:10.1016/j.trb.2005.05.001.

[2] X. Chen, Q. Shi and L. Li, "Location specific cell transmission model for freeway traffic", *Tsinghua Sci. Technol.* **15** (2010) 475–480; doi:10.1016/S1007-0214(10)70090-0.

[3] C. F. Daganzo, "The cell transmission model: a dynamic representation of highway traffic consistent with hydrodynamic theory", *Transport. Res. B-Meth.* **28B** (1994) 269–287; doi:10.1016/0191-2615(94)90002-7.

[4] C. F. Daganzo, "The cell transmission model, part II: network traffic", *Transport. Res. B-Meth.* **29B** (1995) 79–93; doi:10.1016/0191-2615(94)00022-R.

[5] N. Daiheng, *Traffic flow theory: characteristics, experimental methods, and numerical techniques*, (Elsevier, Oxford, 2016) doi:10.1016/C2015-0-01702-6; ISBN: 978-0-12-804134-5.

[6] G. Gomes, R. Horowitz, A. A. Kurzhanskiy, P. Varaiya and J. Kwon, "Behavior of the cell transmission model and effectiveness of ramp metering", *Transport. Res. Part C Emerg. Technol.* **16** (2008) 485–513; doi:10.1016/j.trc.2007.10.005.

[7] R. Haberman, *Mathematical models: mechanical vibrations, population dynamics, and traffic flow* (Prentice Hall, Hoboken, NJ, 1977) doi:10.1137/1.9781611971156.fm.

[8] J. P. Lebacque, "The Godunov scheme and what it means for first order traffic flow models", *Proc. 13th Int. Symp. Transport. Traffic Theory*, Lyon, France 24–26 July, 1996, (Elsevier, Oxford, 1996).

[9] R. J. LeVeque, *Numerical methods for conservation laws*, *Lect. in Math. ETH Zurich.* 1st edn (Springer Basel, Basel, 1990) ISBN 978-3-0348-5116-9; doi:10.1007/978-3-0348-5116-9.

[10] J. Long, Z. Gao, X. Zhao, A. Lian and P. Orenstein, "Urban traffic jam simulation based on the cell transmission model", *Netw. Spat. Econ.* **11** (2011) 43–64; doi:10.1007/s11067-008-9080-9.

[11] L. Muñoz, X. Sun, R. Horowitz and L. Alvarez-Icaza, "Traffic density estimation with the cell transmission model", *Proc. 2003 Amer. Control Conf.*, Denver, CO, 4–6 June 2003, Volume 5 (Institute of Electrical and Electronics Engineers (IEEE), Denver, CO, 2003) 3750–3755; doi:10.1109/ACC.2003.1240418.

[12] G. Orosz, R. E. Wilson and G. Stépán, "Traffic jams: dynamics and control", *Philos. Trans. R. Soc. A* **368** (2010) 4455–4479; doi:10.1098/rsta.2010.0205.

[13] M. Papageorgiou, "Dynamic modelling, assignment and route guidance in traffic networks", *Transport. Res. B-Meth.* **24** (1990) 471–495; doi:10.1016/0191-2615(90)90041-V.

[14] S. R. Pudjaprasetya, J. Bunawan and C. Novtiar, "Traffic light or roundabout? Analysis using the modified kinematic LWR model", *East Asian J. Appl. Math.* **4** (2016) 80–88; doi:10.4208/eajam.210815.281215a.

[15] S. R. Pudjaprasetya and P. Z. Kamalia, "Finite volume method for simulations of traffic dynamics with exits and entrances", *ANZIAM J.* **60** (2018) 1–24; doi:10.21914/anziamj.v60i0.12435.

[16] A. Sumalee, R. X. Zhong, T. L. Pan and W. Y. Szeto, "Stochastic cell transmission model (SCTM): a stochastic dynamic traffic model for traffic state surveillance and assignment", *Transport. Res. B-Meth.* **45** (2011) 507–533; doi:10.1016/j.trb.2010.09.006.

[17] J. Wenlong, *Kinematic wave model of network vehicular traffic* (University of California, Davis, CA, 2003) arXiv:math/0309060.pdf.

[18] H. M. Zhang, N. Yu and Q. Zhen, "Modelling network flow with and without link interactions: the cases of point queue, spatial queue and cell transmission model", *Transportmetrica B* **1** (2013) 33–51; doi:10.1080/21680566.2013.785921.